


 Cite this: *RSC Adv.*, 2022, 12, 16918

# Preparation and performance of chlorfenapyr microcapsules with a degradable polylactide-based polyurethane wall material

 Linfang Zhu,<sup>a</sup> Guangqi Jiang,<sup>b</sup> Jun Cen<sup>a</sup> and Linhui Li<sup>a</sup>

To improve the utilization rate of chlorfenapyr and make the wall material of chlorfenapyr microcapsules easily degradable, polylactide diol, toluene diisocyanate and 1,4-butanediol were used to prepare a chlorfenapyr microcapsule suspension by interfacial polymerization. The product was characterized by the methods of optical microscopy, scanning electron microscopy and Fourier-transform infrared spectroscopy. The results indicated that the microcapsule particles were spherical, with an encapsulation efficiency of 84.20%. The diluted product had good wetting and spreading abilities on cabbage leaves. Compared with other commercial formulations, the slow-release effect of the microcapsule suspension was more obvious and the release mechanisms conform to Fickian diffusion, with the release rate controllable by adjusting the external pH conditions. Furthermore, the wall material of the microcapsules showed good degradation performance in a phosphate-buffered solution. Microencapsulation by this method significantly increased the validity period of chlorfenapyr and the wall material was also degraded easily.

Received 2nd May 2022

Accepted 29th May 2022

DOI: 10.1039/d2ra02787a

[rsc.li/rsc-advances](http://rsc.li/rsc-advances)

## 1 Introduction

Pesticide-based slow and controlled release systems allow the active ingredient of the pesticide to be released continuously and stably, so that the lowest effective level of pesticide can be maintained for a long time.<sup>1</sup> Microencapsulation is a common method used to achieve slow and controlled release performance for many kinds of pesticides, and the slow and controlled release performance is mainly determined by the properties of the active ingredients of the pesticide and the nature of the wall materials of the microcapsules.<sup>2</sup> Microencapsulation of pesticides can reduce the loss of pesticides by volatilization and degradation when exposed to external environments, thereby enhancing the utilization rate and reducing the toxicity of the pesticides.<sup>3</sup> Recently, H. W. An *et al.* fabricated a universal drug delivery platform based on an intracellular self-assembly strategy to achieve effective drug delivery.<sup>4</sup> H. Sawalha *et al.* demonstrated that the properties of the capsules could be optimized through the polymer solidification process, and the choice of appropriate non-solvents and oils can have an important role in the preparation of such capsules.<sup>5</sup>

Polyurethane (PU) is widely used in the fields of medicine,<sup>6–8</sup> pesticides<sup>9</sup> and materials<sup>10</sup> due to its low cost and good thermal stability. PU is also one of the commonly used materials in the

preparation of microcapsules.<sup>11,12</sup> However, PU is difficult to degrade and can pollute soil environments. To develop green and environmentally-friendly pesticide formulations, degradable materials have been used as wall materials for microcapsules and this has become a focus for agricultural chemists.<sup>13,14</sup> Nowadays, it is easily to obtain degradable PU by adding biodegradable substances in its preparation process.<sup>15,16</sup> Among these substances, polylactic acid (PLA) is low cost and has good degradability and biocompatibility. The final products of PLA degradations are CO<sub>2</sub> and H<sub>2</sub>O, which are friendly to humans and the environment, resulting in PLA often being used as a carrier material for drugs and cells in encapsulation fields.<sup>17–20</sup>

Chlorfenapyr is a widely used insecticide and acaricide in vegetables, fruits, and other crops, but damage to crops occasionally occurs in some areas and chlorfenapyr is highly toxic to aquatic organisms, thereby limiting its applications in agriculture.<sup>21–23</sup> Commonly, commercial formulations of chlorfenapyr are microemulsions (ME), emulsifiable concentrates (EC) and other traditional formulations. Its microcapsule suspension with a general PU wall material has rarely appeared in the

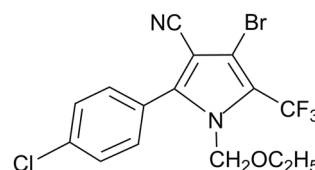


Fig. 1 Structure of chlorfenapyr.

<sup>a</sup>College of Chemistry and Chemical Engineering, Guizhou University, Guiyang, China

<sup>b</sup>State Key Laboratory Breeding Base of Green Pesticide and Agricultural Bioengineering, Key Laboratory of Green Pesticide and Agricultural Bioengineering, Ministry of Education, Guizhou University, Guiyang, China. E-mail: gqjiang@163.com


market and to the best of our knowledge, chlorfenapyr microcapsule suspension (MS) with a degradable PU wall material have not been reported so far. The structure of chlorfenapyr is shown in Fig. 1.

In this study, chlorfenapyr microcapsules were prepared by interfacial polymerization with optimized preparation conditions. The slow-release performance differences between the microcapsule formulation and other commercial formulations were investigated and the release mechanisms were studied. In addition, the wetting and spreading abilities of the diluted microcapsule suspension on the surface of cabbage leaves and the degradation performance of the microcapsule wall material in a phosphate-buffered solution (PBS) solution was also studied. The chlorfenapyr microcapsules showed excellent slow-release, wetting and degradation performance.

## 2 Materials and methods

### 2.1 Materials

Chlorfenapyr was provided by Capot Chemical Co., Ltd (Zhejiang, China) and used as received. Polylactide diol (PLA-500, 500 g mol<sup>-1</sup>) was purchased from Hubei Yisheng New Material Co., Ltd (Hubei, China). Toluene diisocyanate (TDI, 98%, 80/20) was acquired from Meicheng International Trade Co., Ltd (Jiangsu, China). The 1,4-butanediol (BDO) is an analytical reagent and was purchased from the Tianjin Damao Chemical Reagent Factory (Tianjin, China). Stannous octoate (Sn(Oct)<sub>2</sub>, 95%) was provided by Shanghai Tengzhun Biotechnology Co., Ltd (Shanghai, China). Polycarbodiimide was purchased from Dongguan Shunjie Plastic Technology Co., Ltd (Guangdong, China). Agricultural emulsifier 600<sup>#</sup> was bought from Chengdu Jinshan Chemical Reagent Co., Ltd (Sichuan, China). Sodium dodecyl benzene sulfonate (SDBS) was supplied by the Tianjin Beichen Fangzheng Reagent Factory (Tianjin, China). Span 80 and Tween 20 were purchased from the Jiangsu Hai'an Petrochemical Factory (Jiangsu, China). Cyclohexanone, methanol and *n*-hexane, as analytical reagents, were bought from the Aladdin Industrial Corporation (Shanghai, China). 10% chlorfenapyr microemulsion was purchased from Guangdong Zhengze Biological Technology Co., Ltd (Guangdong, China). 10% chlorfenapyr suspension concentrate (SC) was bought from BASF SE Co., Ltd (Ludwigshafen, Germany).

### 2.2 Preparation of chlorfenapyr microcapsules

**2.2.1 Synthesis of PU prepolymer.** The PU prepolymer was synthesized according to the literature procedure.<sup>16,24</sup> As shown in Fig. 2, 19.14 g were dried at 120 °C under a vacuum for 2 h. PLA-500 and 20.00 g TDI were weighed in a 250 mL three-necked flask. The three-necked flask was then placed in a constant temperature water bath under the protection of N<sub>2</sub>. 22.82 g of cyclohexanone and 0.30 g polycarbodiimide were added to the reaction system, at this time, the viscosity of the system was 198.0 mPa s. When the temperature increased to 75 °C, Sn(Oct)<sub>2</sub> (0.3%, wt/wt) was added as a catalyst after 3 h and then reacted for 10 min to obtain the PU prepolymer, the viscosity of the prepolymer increased to 343.0 mPa s.

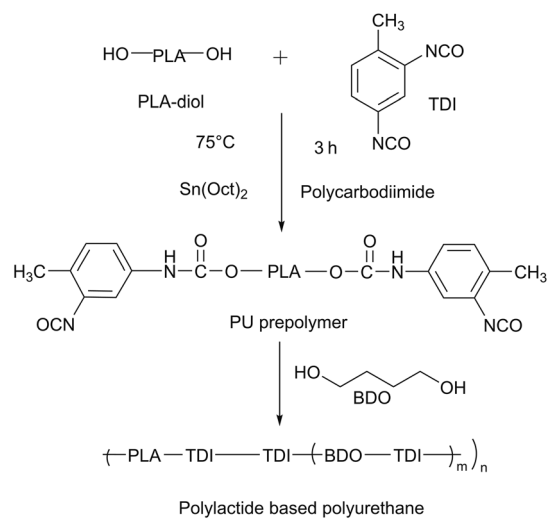


Fig. 2 Synthesis of PU wall material.

**2.2.2 Preparation of chlorfenapyr microcapsules.** The 10.00 g of chlorfenapyr were dissolved in 26.30 g of PU prepolymer to form an oil phase. 1.00 g of agricultural emulsifier 600<sup>#</sup>, 0.49 g of sodium salt of polynaphthalene sulphonic acid and 0.03 g of xanthan gum were dissolved in deionized water to form a water phase. The two phases were mixed and sheared at a high speed of 12 000 rpm to form a uniform O/W emulsion. The emulsion was placed into a 250 mL three-necked flask and 2.95 g of BDO solution were slowly added dropwise at a stirring speed of 600 rpm, before being placed in a 50 °C water bath for constant temperature solidification for 4 h. Finally, the mixture was naturally cooled and a chlorfenapyr microcapsule suspension could be obtained.

### 2.3 Characterization

**2.3.1 Morphological characteristics and elemental distribution of microcapsules.** A small amount of microcapsule suspension was taken and evenly smeared on a glass slide.<sup>25</sup> The preliminary morphology of the microcapsule was analyzed using an OLYMPUS BX43 optical microscope (OM, Olympus Corporation, Japan). The structure and surface morphology of the microcapsule was recorded using SU8020 scanning electron microscopy (SEM, Tianmei Scientific Instruments Co., Ltd, China). The distribution of elements in chlorfenapyr microcapsules was measured with energy dispersive spectroscopy (EDS, Tianmei Scientific Instruments Co., Ltd, China).

**2.3.2 Particle size distribution.** The particle size distribution of the microcapsule suspension was measured by an LS13320 laser particle size analyzer (Beckman, USA).

**2.3.3 Fourier-transform infrared spectroscopy.** An amount of microcapsule suspension was taken, centrifuged, washed and dried. The Fourier-transform infrared (FTIR) spectra of the samples were determined using a VERTEX70 FTIR spectrometer (Brooks, Germany) at a wavelength scan range of 400–4000 cm<sup>-1</sup>.



**2.3.4 Determination of encapsulation efficiency (EE)%.** An amount of chlorfenapyr was dissolved in a methanol solution and the volume was adjusted to 25 mL as a standard solution. An amount of the microcapsule suspension was weighed and placed into a 25 mL volumetric flask and an appropriate amount of methanol was added, and the suspension was then ultrasonically disrupted for 2 h and subsequently diluted to 25 mL with a methanol solution to determine the total content of chlorfenapyr in the microcapsule suspension (LC)%. An amount of the microcapsule suspension was put into a 2 mL centrifuge tube, the suspension was then extracted with hexane three times and the extracts were combined and diluted to 25 mL with a methanol solution to determine the content of chlorfenapyr outside of the microcapsules (X)%. The encapsulation efficiency (EE)% of the microcapsules was calculated by eqn (3).<sup>26</sup>

The chlorfenapyr concentration in the solution was determined using a LC-20A high-performance liquid chromatograph (HPLC, Shimadzu, Japan) with a UV detector, three parallel experiments were conducted for each of the microcapsule samples. The test conditions were methanol/water (92/8, v/v) as a mobile phase with a flow rate of 1 mL min<sup>-1</sup>. The sample injection volume was 5 μL and the detection wavelength was 261 nm.<sup>27</sup> The active ingredients were separated using a Zorbax Eclipse XDB C18 column (4.6 mm × 250 mm, 5 μm, Daicel Investment Co., Ltd, China). The above solutions were filtered with a 0.22 μm nylon 66 filter membrane.

$$(\text{LC})\% = \frac{0.98 \times A_p \times m_y}{m_p \times A_y} \times 100 \quad (1)$$

$$(X)\% = \frac{\text{LC}\% \times m_p \times A_c}{m_c \times A_p} \times 100 \quad (2)$$

$$(\text{EE})\% = \frac{\text{LC} - X}{\text{LC}} \times 100 \quad (3)$$

where  $A_p$  is the peak area of chlorfenapyr in the disrupted microcapsule suspension, mAU,  $A_y$  is the peak area of chlorfenapyr in the standard solution, mAU,  $m_y$  is the mass of chlorfenapyr in the standard solution, g,  $m_p$  is the mass of the disrupted microcapsule suspension, g,  $A_c$  is the peak area of chlorfenapyr in the extraction solution, mAU, and  $m_c$  is the mass of the chlorfenapyr microcapsule suspension for extraction, g.  $X\%$  is the content of chlorfenapyr outside of the microcapsule, LC% is the loading content of the microcapsule.

**2.3.5 Contact angle and surface tension measurements.** The contact angle of the microcapsule suspension was measured as follows. The microcapsule suspension was diluted 500-fold with deionized water. The contact angle of the suspension on the surface of the cabbage leaf was measured with an OCA 25 contact angle measuring instrument (Dataphys Instruments Co., Ltd, China),<sup>28–30</sup> with 2 μL of the solution deposited on the surface of cabbage leaves. The complete droplet profile in the diffusion process was obtained from the digitized image.<sup>31,32</sup>

The surface tension values of the prepolymer, microcapsule and diluted samples were measured by an OCA 25 contact angle

measuring instrument (Dataphys Instruments Co., Ltd, China) and we maintained the measured surface tension value of distilled water at  $72.0 \pm 0.2$  mN m<sup>-1</sup> at the beginning. Each sample was tested in triplicate. The environmental temperature during the measurement was  $25 \pm 2$  °C.

**2.3.6 Measurement of microcapsule release rate.** The slow-release performance was determined by measuring the cumulative release rate of chlorfenapyr from the microcapsule and other commercial formulations. 10% chlorfenapyr microcapsule suspension, 10% chlorfenapyr microemulsions and 10% chlorfenapyr suspension concentrate 0.15 g samples were placed in a dialysis bag with the intercepted molecular weight of 3000, which was immersed in a brown reagent vial containing 400 mL of release medium of a methanol/water (3/2, v/v) solution. The reagent vial was placed on a shaker at 130 rpm. A 1.5 mL of the release medium outside the dialysis bags were collected at different time intervals, and 1.5 mL of the fresh release medium was added to maintain the same volume of release medium. The concentration of chlorfenapyr in the solution was determined by HPLC.

**2.3.7 Release kinetics study.** The release kinetics of the microcapsules were studied as the published literature.<sup>33</sup> The zero-order, first-order, Higuchi and Korsmeyer–Peppas equations were used to fit the release curve of chlorfenapyr in order to study the release mechanism of the active ingredient in the chlorfenapyr microcapsules.

**2.3.8 Degradability study of wall material of microcapsules.** The degradability of the wall material of the microcapsules was measured as follows. The degradation test was carried out in a PBS solution (pH = 7.4) at 37 °C and the surface morphology changes of the microcapsules were observed by SEM.<sup>15,34,35</sup>

## 3 Results and discussion

### 3.1 Screening of preparation conditions

During the preparation of microcapsule suspension, factors such as the emulsifier, core/shell ratio and the ratio of PLA-500 to TDI affected the morphology, encapsulation efficiency and stability of the microcapsule.

**3.1.1 Selection of emulsifier.** Agricultural emulsifier 600<sup>#</sup>, SDBS, Span 80 and Tween 20 were selected as emulsifiers and an O/W emulsion was prepared after high-speed shearing. The

Table 1 Effect of preparation conditions on encapsulation efficiency of microcapsules

Sample	Core/shell	Polycarbodiimide (%)	PLA-500/TDI	Encapsulation efficiency (%)
M1	1 : 1	0	1 : 3	78.48
M2	1 : 2	0	1 : 3	91.83
M3	1 : 3	0	1 : 3	76.60
M4	1 : 4	0	1 : 3	—
M5	1 : 2	0.5	1 : 3	84.20
M6	1 : 2	1	1 : 3	82.25
M7	1 : 2	0.5	1 : 2	84.25



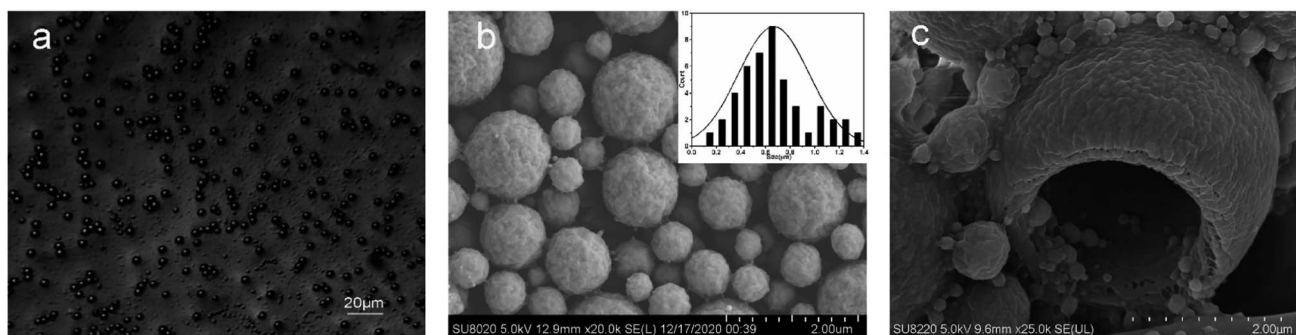


Fig. 3 (a) OM image of microcapsule sample M5. (b and c) SEM images of microcapsule sample M5.

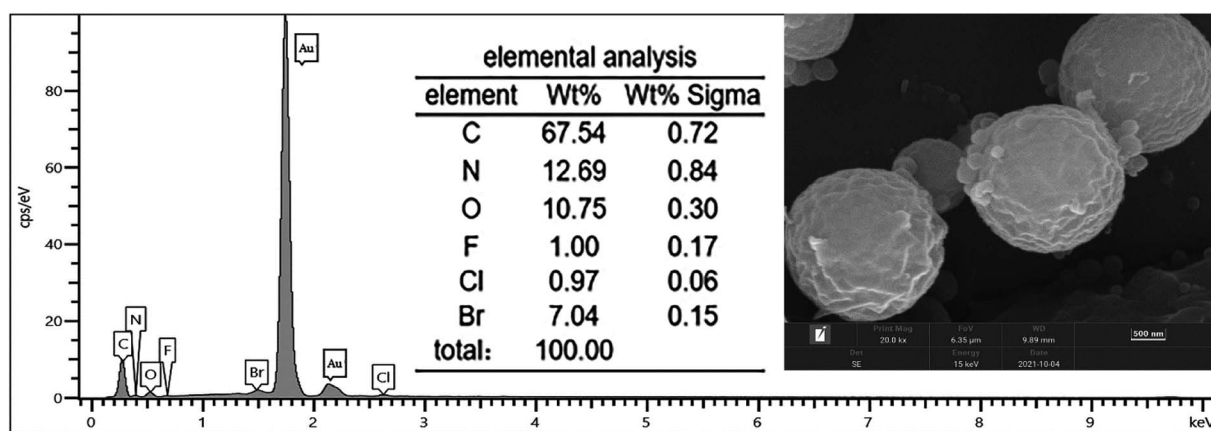


Fig. 4 SEM/EDS image of microcapsule.

morphology of the O/W particles and the stability of the emulsion were observed with an optical microscope. The results showed that when the agricultural emulsifier 600<sup>#</sup> emulsifier was used, the emulsion was stable and the particles were uniform. The emulsion prepared by SDBS could not be dispersed after shearing for 2 min. The emulsion prepared by Span 80 and Tween 20 was relatively stable, but the particles had poor dispersibility and irregular particle morphologies.

**3.1.2 Effect of preparation conditions on encapsulation efficiency of chlorfenapyr microcapsules.** As shown in Table 1, the chlorfenapyr microcapsule suspension was prepared with core/shell ratios of 1 : 1, 1 : 2, 1 : 3 and 1 : 4. When the core/shell ratio was 1 : 1, the formed capsule wall was thinner and the encapsulating effect of chlorfenapyr was 78.48%. When the core/shell ratio was 1 : 2, the encapsulation efficiency of the microcapsules increased to 91.83%. However, as the core/shell ratio continued to decrease, the viscosity of the system increased, resulting in a decrease in the encapsulation efficiency. When the core/wall ratio was 1 : 4, the fluidity of the system was so low that the reaction cannot proceed.

According to the literature, polylactide-based PU materials have good degradation properties.<sup>36,37</sup> The polycarbodiimide can react with the carboxylic acid produced by the hydrolysis of the polyurethane material, which can terminate its self-initiated cracking process, and is often used as a stabilizer for polyurethane materials.<sup>36,38</sup> Our experimental results showed that

the encapsulation efficiency of the microcapsule suspension without a stabilizer was reduced to ~40% within 3 days, while the encapsulation efficiency of the microcapsule suspension was still maintained above 80% after 60 days when 0.5% of stabilizer was added.

As shown in Table 1, the PLA-500/TDI ratio was fixed at 1 : 2 or 1 : 3 to prepare the PU prepolymer. The encapsulation efficiency of the microcapsules reached ~84% when the PLA-500/TDI ratio was 1 : 2 or 1 : 3, but in the case of 1 : 2, there was serious agglomeration phenomenon in the suspension.

Finally, agricultural emulsifier 600<sup>#</sup>, a core/shell ratio of 1 : 2, stabilizer at 0.5% and a PLA-500/TDI ratio of 1 : 3 were selected to prepare the 10% chlorfenapyr microcapsule suspension (sample M5).

### 3.2 Morphology analysis and element analysis

The OM image of the chlorfenapyr microcapsules is shown in Fig. 3(a). It can be seen that the obtained microcapsule had good dispersibility. The SEM images of the microcapsules are shown in Fig. 3(b) and (c). It is clear that the microcapsule particles were spherical and the wall material was relatively dense. Based on SEM image of Fig. 3(b), the particle size distribution of the prepared microcapsules is between 0.19 and 1.32 μm, and the average particle size is 0.667 μm. In Fig. 3(c), some incomplete capsule particles were found, which clearly



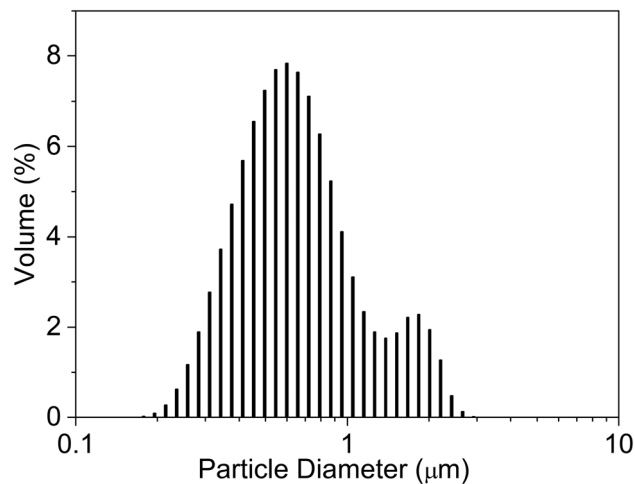


Fig. 5 Particle size distribution of microcapsule sample M5.

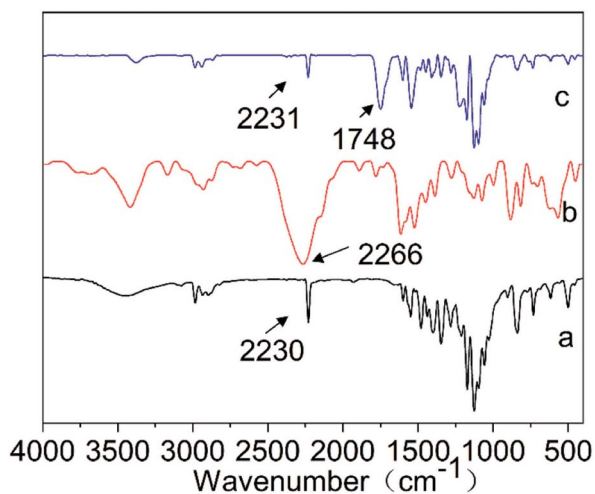


Fig. 6 FTIR spectra of (a) chlorfenapyr, (b) TDI and (c) microcapsule sample M5.

demonstrated the core/shell structure of the microcapsules.<sup>39,40</sup> In order to further verify whether chlorfenapyr is encapsulated in microcapsules, an element mapping analysis was performed using EDS. As shown in Fig. 4, the analysis data showed traces of fluorine, chlorine and bromine, element distribution provided evidence for the successful loading of chlorfenapyr.

### 3.3 Particle size distribution

During the microcapsule formation, the shear forces, interfacial tension and viscous stress have a significant influence on the particle size distribution of microcapsules.<sup>31</sup> The particle size distribution of the microcapsule sample M5 is given in Fig. 5. The average particle size of the microcapsules was 0.8  $\mu\text{m}$ , the average/median ratio was 1.218 and the particle size distribution range was between 0.147 and 2.92  $\mu\text{m}$ . There are two particle size centers for sample M5.

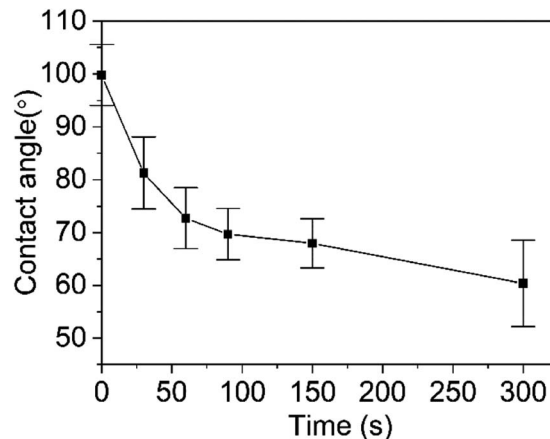


Fig. 7 Contact angle of diluted microcapsule sample M5 on the surface of cabbage leaves.

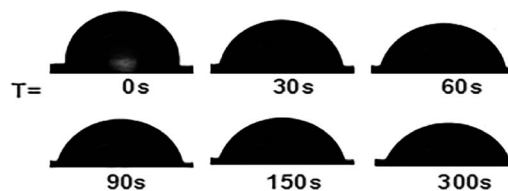


Fig. 8 Droplet shape during wetting.

### 3.4 FTIR spectral analysis

Fig. 6 shows the FTIR spectra of chlorfenapyr, TDI and the microcapsule sample M5. As shown in curve a, the peak at 2230  $\text{cm}^{-1}$  was attributed to the characteristic stretching vibration peak of  $-\text{CN}$  in chlorfenapyr.<sup>41</sup> In curve b, the characteristic absorption peak of  $-\text{NCO}$  of TDI was at 2266  $\text{cm}^{-1}$ .<sup>42,43</sup> In curve c, the characteristic peak of  $-\text{NCO}$  disappeared completely, indicating that the TDI reacted completely in the system and polyurethane was formed.<sup>44,45</sup> The appearance of the characteristic absorption peak at 1748  $\text{cm}^{-1}$  proved that PLA was successfully introduced into the microcapsule wall

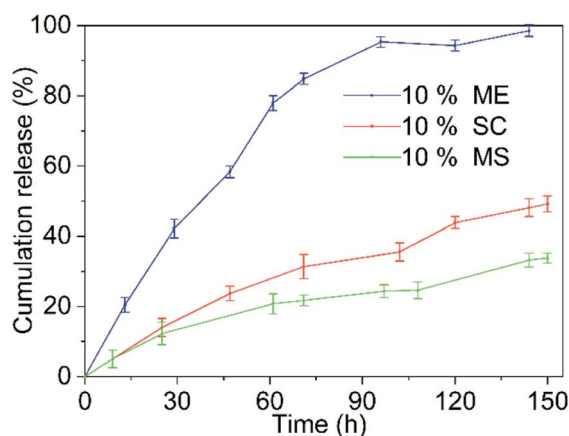


Fig. 9 Release curves of 10% chlorfenapyr ME, 10% chlorfenapyr SC and 10% chlorfenapyr MS.



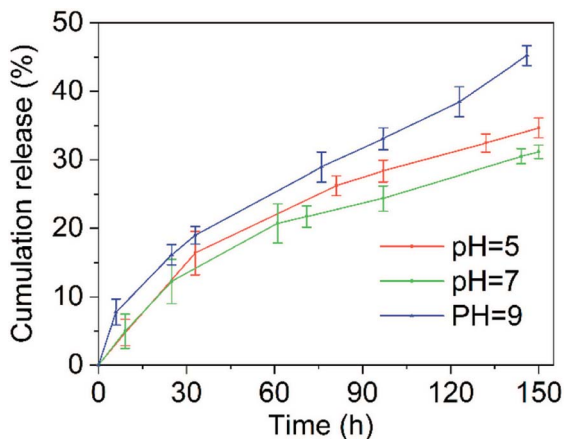


Fig. 10 The release curves for the 10% chlorfenapyr MS in a methanol/water (3/2, v/v) solution with different pH values.

material.<sup>2</sup> The curve c had the characteristic peaks of chlorfenapyr, which proved that chlorfenapyr was successfully encapsulated in the microcapsules.

### 3.5 Contact angle and surface tension analysis

The wetting and spreading abilities of the pesticide formulations on the surface of the crop is often reflected by the contact

angle and  $90^\circ$  is used as the limit of whether the droplets can be wetted on the surface of the leaves.<sup>46,47</sup> Fig. 7 shows the changes of the contact angle of the diluted microcapsule sample M5 on the surface of the cabbage leaf with time. When the droplet was deposited on the leaf surface, the contact angle was  $93.1^\circ$ . Within 30 s, the contact angle of the droplet dropped rapidly to  $79.8^\circ$ . At 300 s, the contact angle decreased to  $68.9^\circ$ . The dynamic change of the droplet shapes during the wetting process is shown in Fig. 8, where it can be seen that the shape of the droplet changed significantly over time. Furthermore, the surface tension values of the prepolymer, microcapsule and diluted samples were measured. The prepolymer is  $3.29 \text{ mN m}^{-1}$ , the chlorfenapyr microcapsule suspension is  $1.98 \text{ mN m}^{-1}$  and the sample diluted 500-fold with deionized water is  $6.13 \text{ mN m}^{-1}$ .

### 3.6 Slow-release performance

The slow-release performance of the microcapsule was determined by factors such as the active ingredients encapsulated in the microcapsules and the nature of the wall material.<sup>35,48</sup> Fig. 9 shows the release curves of the 10% chlorfenapyr microemulsion, 10% chlorfenapyr suspension concentrate and 10% chlorfenapyr microcapsule suspension (microcapsule sample M5), respectively. Among them, the cumulative amount of chlorfenapyr released from the 10% chlorfenapyr

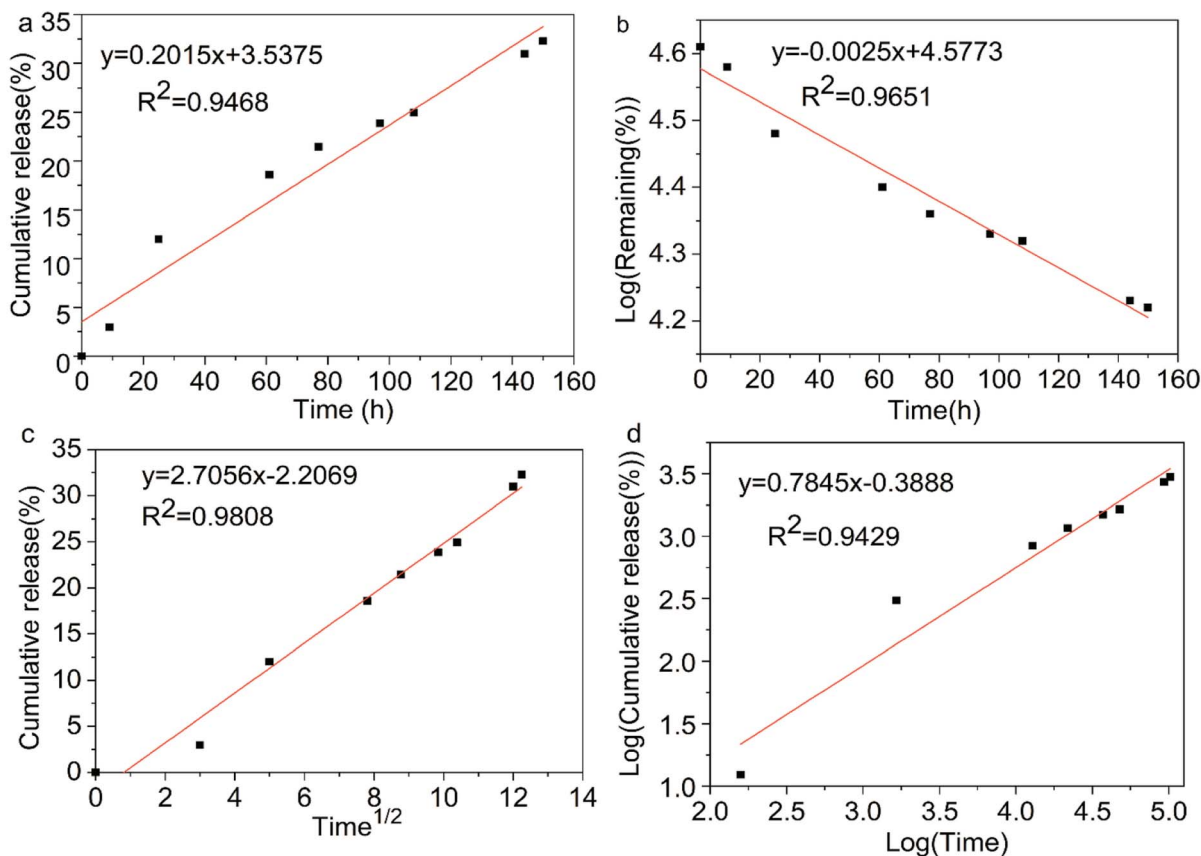


Fig. 11 Kinetic plots of chlorfenapyr microcapsule: (a) zero-order equations; (b) first-order equations; (c) Higuchi equations; (d) Korsmeyer-Peppas equations.



Table 2 Results of microcapsule release kinetics fitting

Kinetic model	Fitted equation	$R^2$
Zero-order	$M_t/M_\infty = 0.2015t$	0.9468
First-order	$\ln(1 - M_t/M_\infty) = 0.0025t$	0.9651
Higuchi	$M_t/M_\infty = 2.7056t^{1/2}$	0.9808
Korsmeyer–Peppas	$M_t/M_\infty = 0.6779t^{0.7845}$	0.9429

microemulsion was 98.57% when the release time was 144 h. The cumulative amount of chlorfenapyr released from the 10% chlorfenapyr suspension concentrate was 49.16% when the time was 150 h. In comparison, the cumulative amount of chlorfenapyr released from the microcapsule sample M5 was much slower, with only 33.80% at 150 h. It can be seen that microencapsulation effectively extended the release time of chlorfenapyr.

Fig. 10 shows the slow-release curves for the 10% chlorfenapyr microcapsule suspension in release media with different pH values. When the other conditions were the same, in release media of pH = 9, the release rate of chlorfenapyr was the fastest because alkaline conditions are most conducive to the hydrolysis of polylactide based polyurethane.<sup>49</sup> Because the hydrolysis of polylactide-based polyurethane under acidic conditions was also faster than in neutral media, the cumulative release rate of chlorfenapyr at pH = 5 was slightly higher than at pH = 7, which was consistent with previous results.<sup>26,50</sup>

### 3.7 Release kinetics of microcapsules

The establishment of the kinetic model can effectively evaluate the release mechanism of the active ingredients in the microcapsules. Commonly used mathematical models for microcapsule formulations are the zero-order, first-order, Higuchi and Korsmeyer–Peppas equations, where  $M_t$  and  $M_\infty$  are the

cumulative release amounts of the drugs at the time of  $t$  and  $\infty$ , respectively.<sup>48</sup> The kinetic plots of chlorfenapyr microcapsule are shown in Fig. 11. Four different kinetic models were used to fit the slow-release curve of the chlorfenapyr microcapsule at pH = 7.<sup>51</sup> The fitting results are shown in Table 2. Among these models, the Higuchi model had the best results. The  $R^2$  value reached 0.9808, which inferred that the release of chlorfenapyr in the microcapsule belonged to Fickian diffusion.

### 3.8 Degradability of wall material of microcapsules

It has been reported in the literature that the ester group was first hydrolyzed in the hydrolysis process of the polylactide based polyurethane material. The carboxylic acid in the product can play a catalytic role and accelerate the degradation of the material.<sup>52</sup> In Fig. 12(a), we provided the hydrolysis mechanism of the ester group on the polylactic acid molecular chain of the polyurethane wall material. Fig. 12(b) shows the SEM image of the original M5 sample. Fig. 12(c) shows the SEM image of the M5 sample after being incubated in PBS and hydrolyzed for 150 h. Fig. 12(d) shows the morphology of microcapsule sample M5 after 12 days incubation in PBS solution. In the case, most of the capsule particles were degraded into fragments, but there were still a few spherical particles. Meanwhile, the viscosity of the system reduced from 562.0 mPa s to 302.3 mPa s, which indirectly revealed the chemical degradation of the wall materials. Comparing Fig. 12(d) with Fig. 12(c), we found that after the microcapsules were incubated in PBS solution for 12 days, the samples showed more fragments.

## 4 Conclusions

Chlorfenapyr microcapsules with degradable polylactide based polyurethane wall material was prepared by interfacial polymerization. This kind of microcapsule possessed high

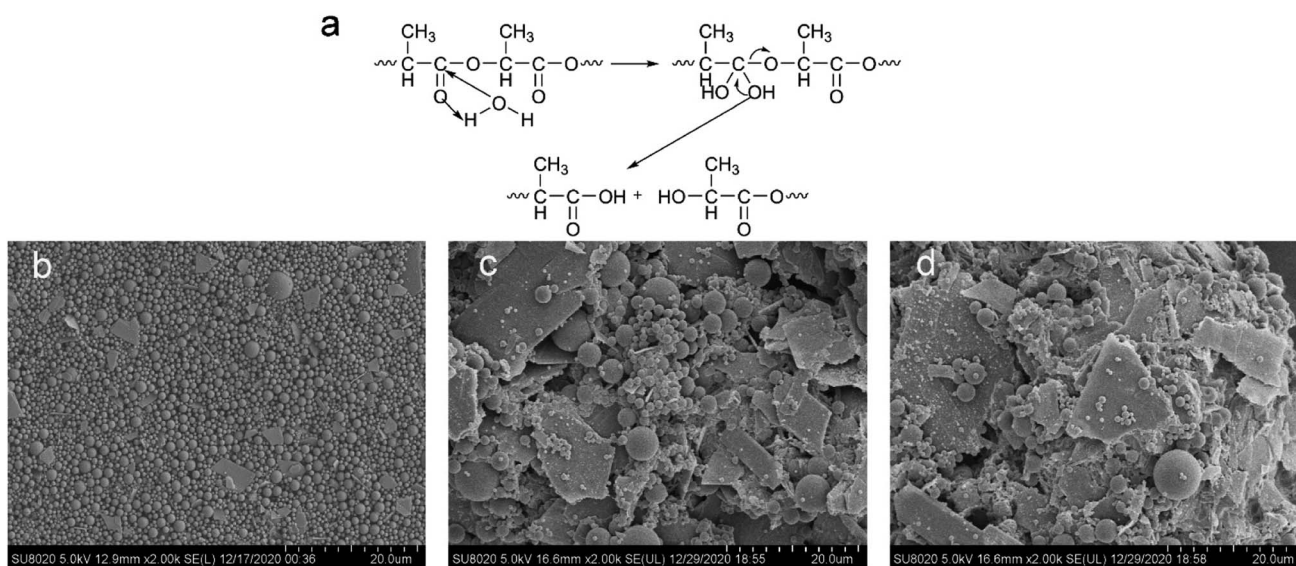


Fig. 12 (a) The hydrolysis mechanism of the ester group on the polylactic acid molecular chain of the polyurethane wall material; (b) SEM image of the original M5 sample; (c) SEM image of the M5 sample after being incubated in PBS for 150 h; (d) the morphology of microcapsule sample M5 after 12 days incubation in PBS solution.



encapsulation efficiency and narrow particle size distribution, and its release mechanisms conformed to Fickian diffusion. Compared with other commercial formulations, chlorfenapyr microcapsules effectively prolonged the release time of chlorfenapyr and the release rate was controlled by adjusting the external pH conditions. The diluted microcapsule formulations had good wetting and spreading abilities on the surface of cabbage leaves. Furthermore, the polylactide-based polyurethane wall material of chlorfenapyr microcapsules showed excellent degradation performance in a PBS solution.

## Conflicts of interest

The authors report there are no competing interests to declare.

## Funding

This work was supported by the opening foundation of the Key Laboratory of Green Pesticide and Agricultural Bioengineering, Ministry of Education, Guizhou University, Grant No. 2016GDGP0102.

## Acknowledgements

We thank International Science Editing (<https://www.internationalscienceediting.com>) for editing this manuscript.

## References

- B. Liu, Y. Wang, F. Yang, X. Wang, H. Shen, H. Cui and D. Wu, *Colloids Surf., B*, 2016, **144**, 38–45.
- T. Zheng, K. Chen, W. Chen, B. Wu, Y. Sheng and Y. Xiao, *J. Microencapsulation*, 2019, **36**(1), 62–71.
- S. Kumar, G. Bhanjana, A. Sharma, M. C. Sidhu and N. Dilbaghi, *Carbohydr. Polym.*, 2014, **101**, 1061–1067.
- H. W. An, M. Mamuti, X. Wang, H. Yao, M. D. Wang, L. Zhao and L. L. Li, *Exploration*, 2021, **1**, 20210153.
- H. Sawalha, K. Schroën and R. Boom, *Chem. Eng. J.*, 2011, **169**, 1–10.
- V. Kanyanta and A. Ivankovic, *J. Mech. Behav. Biomed. Mater.*, 2010, **3**(1), 51–62.
- P. Gentile, D. Bellucci, A. Sola, C. Mattu, V. Cannillo and G. Ciardelli, *J. Mech. Behav. Biomed. Mater.*, 2015, **44**, 53–60.
- X. Liu, S. She, W. Tong and C. Gao, *RSC Adv.*, 2015, **5**(8), 5775–5780.
- E. Rosenbauer, M. Wagner, A. Musyanovych and K. Landfester, *Macromolecules*, 2010, **43**(11), 5083–5093.
- P. F. De Castro and D. G. Shchukin, *Chem.–Eur. J.*, 2015, **21**(31), 11174–11179.
- N. Tsuda, T. Ohtsubo and M. Fuji, *Adv. Powder Technol.*, 2012, **23**(6), 724–730.
- Y. Xu, L. Wang, Y. Tong, S. Xiang, X. Guo, J. Li, H. Gao and X. Wu, *J. Appl. Polym. Sci.*, 2016, **133**(35), 43844.
- Y. Wang, C. Li, T. Wang, X. Li and X. Li, *Langmuir*, 2020, **36**(41), 12336–12345.
- J. Yang, Z. Zhou, Y. Liang, J. Tang, Y. Gao, J. Niu, H. Dong, R. Tang, G. Tang and Y. Cao, *ACS Sustainable Chem. Eng.*, 2020, **8**(35), 13440–13448.
- Y. Xiao, B. Wu, X. Fu, R. Wang and J. Lei, Preparation of biodegradable microcapsules through an organic solvent-free interfacial polymerization method, *Polym. Adv. Technol.*, 2019, **30**(2), 483–488.
- X. Zhao, T. Shou, R. Liang, S. Hu, P. Yu and L. Zhang, *Ind. Crops Prod.*, 2020, **154**, 112619.
- X. Shi, J. Jiang, L. Sun and Z. Gan, *Colloids Surf., B*, 2011, **85**(1), 73–80.
- B. Liu, X. Zhou, F. Yang, H. Shen, S. Wang, B. Zhang, G. Zhi and D. Wu, *Polym. Chem.*, 2014, **5**(5), 1693–1701.
- D. Huang, D. Li, T. Wang, H. Shen, P. Zhao, B. Liu, Y. You, Y. Ma, F. Yang, D. Wu and S. Wang, *Biomaterials*, 2015, **52**, 417–425.
- Y. Duan, B. Zhang, L. Chu, H. H. Tong, W. Liu and G. Zhai, *Colloids Surf., B*, 2016, **141**, 345–354.
- S. Han, S. Yeom, S. Lee, S. C. Park, H. B. Kim, Y. M. Cho and S. W. Park, *Hong Kong J. Emerg. Med.*, 2019, **26**(6), 375–378.
- A. A. Romeh and R. A. Ibrahim Saber, *J. Environ. Manage.*, 2020, **260**, 110104.
- A. Younas, H. N. Rashid, D. Hussain, S. T. R. Naqvi, M. Ali Khan, B. Fatima and S. Majeed, *J. Environ. Manage.*, 2021, **284**, 112017.
- M. Kaur, K. M. Gupta, A. E. Poursaid, P. Karra, A. Mahalingam, H. A. Aliyar and P. F. Kiser, *Drug Delivery Transl. Res.*, 2011, **1**(3), 223–237.
- F. Yu, Y. Wang, Y. Zhao, J. Chou and X. Li, *Materials*, 2021, **14**(13), 3753.
- R. Wang and Y. Xiao, *J. Appl. Polym. Sci.*, 2019, **137**(16), 48594.
- Y. Cao, J. Chen, Y. Wang, J. Liang, L. Chen and Y. Lu, *Sci. Total Environ.*, 2005, **350**(1–3), 38–46.
- C. Cao, Y. Song, Z. Zhou, L. Cao, F. Li and Q. Huang, *Soft Matter*, 2018, **14**(39), 8030–8035.
- B. Liu, Y. Fan, H. Li, W. Zhao, S. Luo, H. Wang, B. Guan, Q. Li, J. Yue, Z. Dong, Y. Wang and L. Jiang, *Adv. Funct. Mater.*, 2021, **31**, 2006606.
- T. Wu, X. Fang, Y. Yang, W. Meng, P. Yao, Q. Liu, B. Zhang, F. Liu, A. Zou and J. Cheng, *J. Agric. Food Chem.*, 2020, **68**, 12549–12557.
- M. Li, W. Xu, D. Hu and B. Song, *Colloids Surf., A*, 2018, **553**, 578–585.
- T. Wu, X. Fang, Y. Yang, W. Meng, P. Yao, Q. Liu, B. Zhang, F. Liu, A. Zou and J. Cheng, *J. Agric. Food Chem.*, 2020, **68**(45), 12549–12557.
- S. Likhitkar and A. K. Bajpai, *Carbohydr. Polym.*, 2012, **87**(1), 300–308.
- S. Xue, D. Pei, W. Jiang, Y. Mu and X. Wan, *Polymer*, 2016, **99**, 340–348.
- J. Luo, X. Huang, T. F. Jing, D. X. Zhang, B. Li and F. Liu, *ACS Sustainable Chem. Eng.*, 2018, **6**(12), 17194–17203.
- J. G. Kennemur and B. M. Novak, *Polymer*, 2011, **52**(8), 1693–1710.
- S. Chen, C. Ma and G. Zhang, *Prog. Org. Coat.*, 2017, **104**, 58–63.





- 38 Z. Lu, W. Guan and L. Tang, *Prog. Org. Coat.*, 2019, **132**, 328–335.
- 39 J. Zhou, W. Xu, Y. Wang and B. Shi, *RSC Adv.*, 2017, **7**(34), 21196–21204.
- 40 F. Zhang, T. Zhao, D. Ruiz-Molina, Y. Liu, C. Roscini, J. Leng and S. K. Smoukov, *ACS Appl. Mater. Interfaces*, 2020, **12**(41), 47059–47064.
- 41 N. Abbas, M. Hayat, H. Fatima, S. Manzoor, S. Nawaz, F. Mabood, G. Yasmean, A. Majeed and S. Manzoor, *Sep. Sci. Technol.*, 2021, **56**(3), 518–526.
- 42 Z. Zhang, H. Song, X. Men and Z. Luo, *Wear*, 2008, **264**(7–8), 599–605.
- 43 J. Kim, T. S. Pathak, J.-H. Yun, K.-P. Kim, T.-J. Park, Y. Kim and K.-J. Paeng, *J. Polym. Environ.*, 2013, **21**(1), 224–232.
- 44 P. K. S. Pillai, S. Li, L. Bouzidi and S. S. Narine, *Ind. Crops Prod.*, 2016, **83**, 568–576.
- 45 S. Zhan, S. Chen, L. Chen and W. Hou, *Powder Technol.*, 2016, **292**, 217–222.
- 46 V. Starov, N. Ivanova and R. G. Rubio, *Adv. Colloid Interface Sci.*, 2010, **161**(1–2), 153–162.
- 47 N. A. Ivanova and V. M. Starov, *Curr. Opin. Colloid Interface Sci.*, 2011, **16**(4), 285–291.
- 48 C. G. England, M. C. Miller, A. Kuttan, J. O. Trent and H. B. Frieboes, *Eur. J. Pharm. Biopharm.*, 2015, **92**, 120–129.
- 49 D. K. Chattopadhyay and K. V. S. N. Raju, Structural engineering of polyurethane coatings for high performance applications, *Prog. Polym. Sci.*, 2007, **32**(3), 352–418.
- 50 S. Motokucho, Y. Nakayama, H. Morikawa and H. Nakatani, *J. Appl. Polym. Sci.*, 2018, **135**(8), 45897.
- 51 Y. Xu, R. Zhao, H. Chen, X. Guo, Y. Huang, H. Gao and X. Wu, *J. Polym. Res.*, 2021, **28**(1), 1–11.
- 52 D. Macocinschi, D. Filip, M. F. Zaltariov and C. D. Varganici, *Polym. Degrad. Stab.*, 2015, **121**, 238–246.

